



Published in final edited form as:

Cancer. 2009 July 15; 115(14): 3360–3368. doi:10.1002/cncr.24371.

Targeting the Urokinase Plasminogen Activator Receptor With a Monoclonal Antibody Impairs the Growth of Human Colorectal Cancer in the Liver

George Van Buren II, MD¹, Michael J. Gray, MD¹, Nikolaos A. Dallas, MD¹, Ling Xia, MD², Sherry J. Lim, MD¹, Fan Fan, MD², Andrew P. Mazar, PhD³, and Lee M. Ellis, MD^{1,2}

¹Department of Surgical Oncology, The University of Texas M. D. Anderson Cancer Center, Houston, Texas

²Department of Cancer Biology, The University of Texas M. D. Anderson Cancer Center, Houston, Texas

³Attenuon, LLC, San Diego, California

Abstract

BACKGROUND—Urokinase plasminogen activator receptor (uPAR) expression has been shown to correlate with poor prognosis in colorectal cancer (CRC). The authors hypothesized that targeting uPAR, a receptor involved in cell proliferation, migration, invasion, adhesion, and angiogenesis, would impair the growth of CRC in the liver, the most common site of metastasis.

METHODS—Human CRC cell lines were examined for uPAR expression by Western blot analysis. The in vitro effects of the uPAR monoclonal antibody (MoAb) (ATN-658) were tested in proliferation and migration assays. For in vivo studies, human HCT116 CRC cells were injected directly into the livers of mice in 2 separate studies, the first to determine the effect of therapy with ATN-658 on small-volume disease (therapy begun on Day 4), and a second study to determine the effect of therapy on established disease (therapy begun on Day 12). Mice were randomized to receive either nonspecific immunoglobulin G MoAb (control) or ATN-658, and were sacrificed 1 month after tumor implantation.

RESULTS—uPAR was expressed by all CRC cell lines studied. In vitro, ATN-658 had minimal effect on CRC proliferation in monolayers, but significantly decreased CRC cell migration. In vivo, ATN-658 led to significant reductions in tumor growth versus control when initiated either 4 or 12 days after tumor implantation (–65% vs control [$P = .05$] and –85% vs control [$P = .05$]). ATN-658 significantly inhibited in vivo tumor cell proliferation in both studies.

CONCLUSIONS—uPAR MoAb therapy impaired CRC tumor growth in the liver in both small-volume and large-volume disease models.

Corresponding author: Lee M. Ellis, MD, Department of Surgical Oncology, Unit 444, The University of Texas M. D. Anderson Cancer Center, PO Box 301402, Houston, TX 77230-1402; Fax: (713) 792-4689; lellis@mdanderson.org. The first 2 authors contributed equally to this article.

Conflict of Interest Disclosure

Supported by US National Institutes of Health grants T-32 09599 (to G.V.B., N.A.D, and S.J.L) and Attenuon, LLC (A.P.M.).

Keywords

anti-urokinase plasminogen activator receptor; metastasis; colorectal cancer; targeted therapy

Colorectal carcinoma (CRC) is the second leading cause of cancer-related deaths in the United States, with approximately 55,000 deaths each year.¹ The current first-line therapy for metastatic CRC (mCRC), including the combination of chemotherapy with monoclonal antibodies (MoAbs) to vascular endothelial growth factor or the epidermal growth factor receptor, leads to median survival of <2 years.^{2,3} New strategies to improve our systemic regimens for mCRC are necessary to further improve outcomes for this disease.

The urokinase plasminogen activator (uPA) ligand and uPA receptor (uPAR) system mediate tumor cell proliferation, adhesion, migration, and invasion.^{4–8} uPAR is a multifunctional cell surface glycosyl phosphatidylinositol–linked protein that engages in numerous protein-protein interactions, and is an important facilitator of the proteolytic cascade involved in tumor invasion and tissue remodeling.⁸ uPA/uPAR expression has been shown to correlate with poor prognosis in various malignancies,^{9–11} including CRC,^{12–17} in which where uPAR is overexpressed.^{7,15,18} uPA and uPAR are involved in CRC cell migration and invasion,^{7,18} and antibodies or antisense to uPAR decreases invasion and metastasis.^{8,19,20} The unique characteristics of the uPAR system make this receptor a potential target for the development of therapies for mCRC. We hypothesized that targeting uPAR will impair CRC growth in 2 distinct phases of tumor growth in the murine liver.

MATERIALS AND METHODS

Reagents

MoAbs to human uPAR (ATN-658) and nonspecific MoAbs were provided by Attenuon, LLC (San Diego, Calif). ATN-658 is a novel human uPAR-specific MoAb that does not inhibit the binding of uPA to uPAR; thus it can bind to uPAR regardless of whether it is occupied by uPA. In addition, ATN-658 can bind to the residual fragment of uPAR frequently observed in tumors that remains attached to the membrane after proteolysis.

Antibodies used for immunohistochemical (IHC) and Western blot analyses were as follows: antibromodeoxyuridine (BrdU) and anti-CD105 antibody (BD Biosciences, San Jose, Calif); anti–proliferating cell nuclear antigen (PCNA) PC-10 (DAKO, Carpinteria, Calif); anti-uPAR (American Diagnostica Inc., Stamford, Conn); and cleaved caspase-3 (BioCare Medical LLC, Concord, Calif).

Cell Lines and Cell Culture Conditions

The human CRC cell lines HCT116, GEO, HT29, RKO, and SW480 were obtained from American Type Culture Collection (Manassas, Va). KM12 was the kind gift of I.J. Fidler, DVM, PhD, of the University of Texas M. D. Anderson Cancer Center. Cells were cultured and maintained in minimum essential medium (MEM) supplemented with 10% fetal bovine serum (FBS), 2 U/mL of a penicillin-streptomycin mixture (Flow Laboratories, Rockville, Md), vitamins (Life Technologies, Inc., Grand Island, NY), 1 mmol/L of sodium pyruvate, 2

mmol/L of L-glutamine, and nonessential amino acids and incubated in 5% carbon dioxide of 95% air at 37°C. In vitro experiments were performed when cells were at 50% to 70% confluence.

Immunoprecipitation and Western Blot Analysis

Whole-cell protein was isolated from CRC cells at 70% to 80% confluence by using RIPA “B” protein lysis buffer as previously described.²¹ The isolated protein was quantified by a commercially available modified Bradford assay (Bio-Rad Laboratories, Hercules, Calif). Cell extracts (in a Triton X-100 buffer with protease inhibitors) were immunoprecipitated with a polyclonal anti-uPAR antibody. The RKO cell line served as the positive control for uPAR.²² The immunoprecipitated material was subjected to Western blot analysis, and the blot was probed with 5 µg/mL of an anti-uPAR MoAb generated against domain 1 of the protein (American Diagnostica, Greenwich, Conn) and a horseradish peroxidase–conjugated goat antimouse immunoglobulin (Ig) G. Protein bands were observed by using a commercially available enhanced chemiluminescence kit (Amersham Biosciences, Fairfield, Conn).

Transwell Migration and Invasion Assays

To assess cell migration in vitro, HCT116, RKO, and SW480 cells (1×10^5 cells in 500 µL MEM supplemented with 1% FBS) were placed in the top chamber of transwell migration chambers (8 µm BioCoat Control Inserts, Becton Dickinson Labware, Bedford, Mass). GEO, HT29, and KM12 cells were not included, because they migrate poorly in in vitro assays. The lower chamber was filled with 750 µL MEM supplemented with 10% FBS plus either nonspecific MoAb (50 µg/mL) or ATN-658 (50 µg/mL). After either 24 or 48 hours, unmigrated cells were removed from the upper surface of the transwell membrane with a cotton swab, and migrated cells on the lower membrane surface were fixed, stained, photographed, and counted under high-power magnification ($\times 100$). HCT116 cells were examined at 24 hours because of rapid migration, and RKO and SW480 cells were examined at 48 hours. Three wells were studied per group, and photographs were taken from 3 random fields of each well.

Cell Counts

The growth rate of HCT116, HT29, RKO, and SW480 cells in the presence of nonspecific MoAb or ATN-658 was evaluated with a 3-(4,5-dimethylthiazol-2-yl)-2,5-diphenyltetrazolium bromide (MTT) assay as follows. Cells (3×10^3) were plated in 96-well plates in MEM with 10% FBS overnight, and the medium was changed the next morning to fresh MEM with 10% FBS with either nonspecific MoAb (50 µg/mL) or ATN-658 (50 µg/mL). All assays were performed in 10 wells per cell line. After 24 hours and 48 hours, 2 mg/mL MTT (Sigma-Aldrich, St. Louis, Mo) in PBS was added (50 µL/well), and plates were incubated at 37°C for 2 hours. At that time, the medium and MTT were removed, dimethyl sulfoxide was added for 10 minutes, and absorbance was measured at 570 nm.

Orthotopic Tumor Model

Six-week-old male nude mice were purchased from the Animal Production Program of the National Cancer Institute's Frederick Cancer Research and Development Center (Frederick, Md) and housed and maintained in accordance with the standards of the University of Texas M. D. Anderson Cancer Center Institutional Animal Care and Use Committee.

HCT116 cells were grown to 80% confluence and trypsinized, and >90% cell viability was confirmed by trypan blue exclusion. Briefly, after anesthesia was induced with ketamine (Sigma, 30 mg/kg intraperitoneally [ip]), an upper midline abdominal incision was created. The left upper liver lobe was isolated, and 1×10^6 cells/50 μ L/mouse were injected beneath the liver capsule. After the injection, pressure was held at the injection site with a sterile cotton swab dipped in ethanol. The wound was closed with staples.

Two separate studies were done to determine the effect of ATN-658 on 1) small-volume disease (therapy begun on Day 4), and 2) established disease (therapy begun on Day 12).

In Study 1, mice were randomly assigned to 1 of 2 groups of 10 and treated with equal-volume ip injections of either nonspecific IgG (10 mg/kg) or ATN-658 (10 mg/kg). Therapy was initiated on Day 4. Antibodies were administered ip twice per week, and treatment was continued until the mice were sacrificed on Day 28.

In Study 2, mice were randomly assigned to 1 of 2 groups of 12 and treated with equal-volume ip injections of either nonspecific IgG (10 mg/kg) or ATN-658 (10 mg/kg). HCT-116 cells were inoculated and allowed to grow for 11 days before initiating treatment. One mouse died during anesthesia induction before injection. Tumors removed after euthanasia on Day 11 from a satellite group of mice ($n = 3$) had a mean tumor volume of approximately 450 mm³. Treatments were initiated the next day (Day 12) in the remaining mice ($n = 10$ per group). Subsequently, antibodies were given ip twice per week, and treatment was continued until the mice were sacrificed on Day 29.

On the day of sacrifice, mice were injected ip with 0.2 mL (50 mg/mL) BrdU (Upstate, Temecula, Calif) 4 hours before being euthanized to assess tumor cell proliferation. Mice were anesthetized by carbon dioxide. Mouse tumors and livers were excised, weighed, and measured. Tumors were measured with calipers, and tumor volumes (in cubic millimeters) were calculated as $(\text{length} \times 0.5) \times \text{width}^2$. A portion of each tumor was placed in 10% formalin (for paraffin embedding), snap-frozen, and placed in Optimal Cutting Temperature solution (Miles Laboratories/Bayer AG, Elkhart, Ind) in preparation for subsequent IHC analyses. The combined liver and tumor weights were collected and normalized to mouse body weights. The tumor volumes for each group were averaged.

Tissue Staining and Immunohistochemistry

Optimum cutting temperature solution (OCT)-embedded liver tissue specimens were fixed in cold acetate for 5 min, acetate+chloroform (1:1) for 5 min, and fresh cold acetate for another 5 min, and IHC staining for BrdU, PCNA, or caspase-3 was performed as previously described.²³ The number of BrdU-positive cells, PCNA-positive cells, or caspase-3-positive

cells were counted in 7 random fields from 5 different tumor specimens per group (magnification, $\times 100$).

Tumor microvascular counts and tumor vessel area were analyzed by IHC. Because the sinusoidal vascular architecture of the liver makes obtaining accurate blood vessel counts difficult, we stained livers for CD105, a marker of activated endothelium, to macroscopically assess the relative levels of activated endothelium among different groups. Slides were fixed in acetone, then endogenous peroxidases were blocked with H_2O_2 in methanol. After antigen retrieval in ethylenediamine tetraacetic acid, slides were blocked with protein-blocking agent for 20 minutes. Then the primary CD105 antibody was added in a 1:100 concentration overnight at $4^\circ C$. After a second protein blockade, specimens were incubated with horseradish peroxidase-conjugated secondary antibody for 30 minutes at room temperature. Slides were observed in the standard fashion. An investigator blinded to treatment group assignment visually compared stained tumors from the various groups.

To evaluate apoptosis, in addition to the caspase-3, the terminal deoxynucleotide transferase-mediated deoxyuridine triphosphate nick-end labeling (TUNEL) assay was performed with a commercial kit (Promega, Madison, Wis) according to the manufacturer's protocol, and counterstained with the DNA-specific dye Hoechst 33,345 (Molecular Probes, Eugene, Ore). The number of TUNEL-stained cells per high-power field was counted in 5 fields per tumor. Fluorescently labeled cells were examined using a Nikon Microphot-FXA fluorescent microscope, and representative images were recorded.

Paraffin-embedded Sections of the Liver

CRC tumors were stained with hematoxylin and eosin (H&E) by standard methods. H&E-stained sections were evaluated under high-power magnification for differences in microscopic architectural changes.

Statistical Analyses

Statistical analyses were done using InStat 3.01 software (GraphPad Software, Inc., San Diego, Calif). The significance of differences between treatment groups and control groups was determined using the Mann-Whitney *U* test, Student *t* test, or Fisher exact test, as appropriate. Significance was determined with 95% confidence intervals.

RESULTS

In Vitro Studies

Expression of uPAR in human CRC cell lines—By immunoprecipitation and Western blot analysis, uPAR expression was present in all human CRC cell lines studied. The RKO cell line is known to express uPAR and served as a positive control (Fig. 1A).²²

Effect of anti-uPAR MoAb on cell proliferation in vitro—To determine the effect of ATN-658 on CRC proliferation in vitro, we performed the MTT assay on HCT116, RKO, SW480, and HT29 cells. At 24 hours, ATN-658 led to a 12% decrease ($P < .05$) in cell proliferation in HCT116 cells, an 8% decrease ($P < .05$) in proliferation in HT29 cells, and

no change in RKO or SW480 cellular proliferation. At 48 hours, ATN-658 led to a 4% decrease ($P < .05$) in cell proliferation in vitro in RKO cells as compared with control, and no change in HCT116, HT29, or SW480 cellular proliferation (data not shown)

Effect of anti-uPAR MoAb on cell migration in vitro—Transwell migration assays were done to evaluate the effect of anti-uPAR therapy on HCT116, RKO, and SW480 cell migration. HCT116 cells were examined at 24 hours, and RKO and SW480 cells were examined at 48 hours. Treatment of cells with ATN-658 led to an approximately 50% inhibition of migration in HCT116 cells, 90% reduction in RKO cells, and 35% reduction in SW480 cells relative to control ($P < .0001$; $P < .0001$; $P < .01$ vs nonspecific IgG MoAb, respectively) (Fig. 1B).

In Vivo Studies

Effect of uPAR MoAb on tumor growth in an orthotopic murine model of CRC growth in the liver

Experiment 1: In the first study, we sought to determine the effects of uPAR blockade on early phases of tumor growth soon after tumor cell implantation in the liver (small-volume disease). When therapy was initiated on Day 4 after tumor cell implantation, ATN-658 inhibited tumor growth by 65% versus nonspecific MoAb control ($P = .05$) (Figs. 2A and 2B).

Experiment 2: In the follow-up study, we sought to determine the effects of uPAR blockade on the growth of established tumors in the liver (large-volume disease). A satellite group of mice ($n = 3$) were euthanized on Day 11 and had a mean tumor volume of approximately 450 mm³. When therapy was initiated on Day 12 on the remaining mice, we observed a more pronounced effect than in the prior experiment, whereby ATN-658 inhibited tumor growth by approximately 85% versus nonspecific MoAb control ($P < .05$) (Fig. 2C).

Effect of uPAR MoAb on tumor cell proliferation—BrdU and PCNA IHC analysis was performed on the human CRC xenografts from the early and late therapy groups to assess in vivo cellular proliferation (Fig. 3). In both experiments, numerous proliferating cells were observed in the nonspecific MoAb-treated tumors. In the early therapy group, the ATN-658 group showed a nearly 60% inhibition of proliferating cells per high-power field as compared with those tumors from mice treated with the nonspecific control MoAb ($P < .002$) (Fig. 3A). In the late therapy group, the ATN-658 group showed a nearly 88% inhibition of proliferating cells per high-power field as compared with those tumors from mice treated with the nonspecific control MoAb ($P < .00002$) (Fig. 3C). The results of the BrdU staining (Fig. 3B and D) were confirmed by PCNA staining (data not shown).

Effect of uPAR MoAb on in vivo apoptosis—To evaluate the effect of ATN-658 on tumor cell apoptosis in vivo, tumor sections were stained for TUNEL-positive cells and caspase-3-positive cells. There was no difference in apoptosis between the control and ATN-658 group in both the early and late experiment (data not shown).

Effect of uPAR MoAb on the tumor-associated vasculature—uPAR has been shown to mediate angiogenesis via regulation of upstream angiogenic mediators.^{4,24} CD105 was used as a marker of activated endothelium.^{25,26} Because the ATN-658 recognizes only uPAR and not murine uPAR, any changes in angiogenesis would be because of an upstream effect on human tumor cells. CD105 staining was done on tumors from the early therapy group, and there was no difference in vessel counts or vessel morphology between the 2 groups (data not shown).

Effect of uPAR MoAb tumor morphology—Light microscopic analysis of H&E-stained sections of the HCT116 tumor xenograft specimens from both the early and late experiment were examined. In both experiments, anti-uPAR therapy did not induce any discernable changes in regard to tumor morphology (data not shown).

DISCUSSION

uPAR expression has been shown to correlate with poor prognosis in CRC.^{12–14,16,17,26} uPAR's primary role in proteolysis, cell migration, growth control, and tumor cell dormancy make it an important mediator of CRC progression and metastasis.^{4,7,18,22} We have previously demonstrated that ATN-658 significantly inhibited pancreatic cancer growth, invasion, and metastasis in an orthotopic xenograft model.⁵ On the basis of uPAR's role in CRC progression, we sought to investigate uPAR as a target in CRC in the liver.

In the first portion of our study, we established that our target uPAR was present in CRC cell lines. Next we assessed the effect of ATN-658 in vitro. The results indicating that ATN-658 inhibited cellular migration and invasion were consistent with what has been shown with uPAR inhibition in CRC and other cell lines in vitro.^{5,18} Although uPAR has been shown to affect proliferation in some tumor cell lines,²⁷ we found that ATN-658 had only minimal effects on tumor cell proliferation in our CRC cells in vitro. This effect on proliferation in vitro was relatively small (0% to 12%) in comparison to the large decrease in proliferation observed in vivo (55% to 90%). This discrepancy is difficult to explain. Of course, in vitro conditions do not mirror the tumor microenvironment in vivo. Although uPAR may inhibit tumor angiogenesis indirectly by down-regulation of tumor cell-derived angiogenic factors, the decrease in tumor cell proliferation observed in vivo was independent of changes in angiogenesis (vessel count). Our in vitro studies were performed in monolayer cultures, and these 2-dimensional studies clearly do not reflect the complexities of the tumor microenvironment. Because ATN-658 does not recognize murine uPAR, effects of ATN-658 cannot directly alter the tumor microenvironment. However, it is possible that ATN-658 can alter secretion of factors from tumor cells that can alter the extracellular matrix. Inhibition of tumor cell migration by ATN-658 was the most marked finding in vitro. We hypothesize that the decrease in tumor cell proliferation observed in vivo is a combination of a small direct effect on tumor cells as well as an indirect effect by ATN-658 on the interaction between the tumor cell and the extracellular matrix.

ATN-658 significantly decreased tumor growth in both small-volume and large-volume disease in the liver. In CRC, uPAR's role in tumor growth is currently being elucidated.^{4,22} In addition, uPAR's biologic cross-talk with other tyrosine kinase systems such as the

HGF/c-MET axis has been shown to play a large role in hepatocellular carcinoma invasion and spread in the liver.²⁸ On the basis of uPAR's role in mediating tumor cell growth^{5,27} and uPAR's role in the liver microenvironment,²⁸ we wanted to assess the affects of targeting uPAR in both small-volume and large-volume colon cancer growth in the liver. We chose the direct liver injection model to study CRC tumor growth in the liver, because this produces a single liver mass that can be easily measured. This model allows us to directly assess CRC tumor growth in the liver, and has been well described in other publications.^{29–31} This model avoids the problems that tend to arise in mCRC models to the liver, such as splenic injections that may have inconsistent tumor take in the liver, ectopic metastasis at the injection sites, and the challenge of quantifying the number of metastases versus growth of individual metastasis. We focused on HCT-116 cells because this cell line produces consistent results when injected in the livers of nude mice.

As in most preclinical studies evaluating therapeutic agents, we initially targeted mCRC in small-volume disease. After we found efficacy at this stage of tumor growth, we subsequently tested our agent in large-volume disease and found similar efficacy. The findings that ATN-658 impaired tumor cell proliferation, but not apoptosis or angiogenesis, suggest that uPAR potentially plays a role in the tumor cell cycle. These results provide a rationale for targeting uPAR for CRC growing in the liver.

Despite improvements with current first-line therapy for mCRC, the median overall survival for patients with mCRC is approximately 20 months, and thus new targeted therapeutics are necessary to further improve treatment options in the field. The results of the current study demonstrate the importance of uPAR in CRC tumor growth and supports further study of uPAR as a therapeutic target for the treatment of CRC.

Acknowledgments

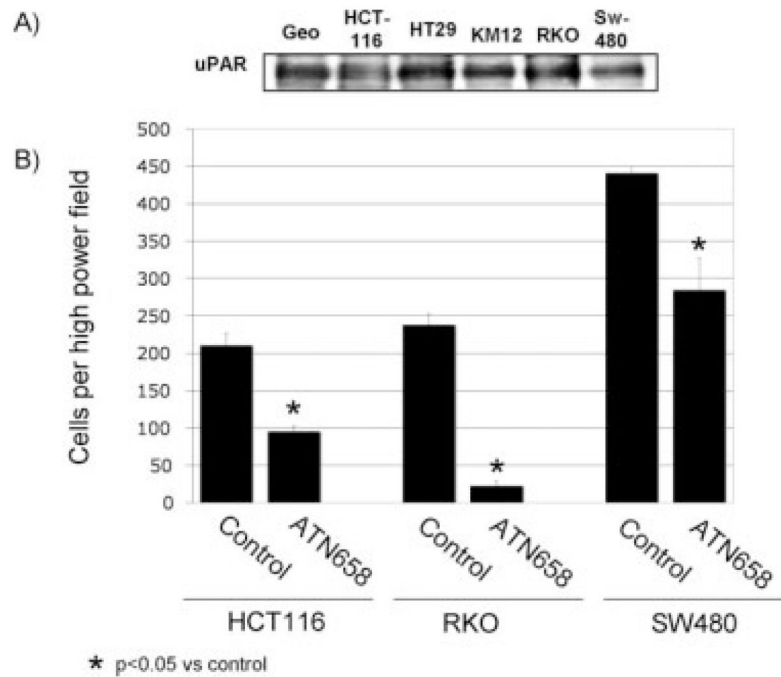
We thank Rita Hernandez, Department of Surgical Oncology, The University of Texas M. D. Anderson Cancer Center, for editorial assistance.

References

1. Jemal A, Siegel R, Ward E, Murray T, Xu J, Thun MJ. Cancer statistics, 2007. *CA Cancer J Clin.* 2007; 57:43–66. [PubMed: 17237035]
2. Abdalla EK, Adam R, Bilchik AJ, Jaeck D, Vauthey JN, Mahvi D. Improving resectability of hepatic colorectal metastases: expert consensus statement. *Ann Surg Oncol.* 2006; 13:1271–1280. [PubMed: 16955381]
3. Bilchik AJ, Poston G, Curley SA, et al. Neoadjuvant chemotherapy for metastatic colon cancer: a cautionary note. *J Clin Oncol.* 2005; 23:9073–9078. [PubMed: 16361615]
4. Mazar AP. Urokinase plasminogen activator receptor choreographs multiple ligand interactions: implications for tumor progression and therapy. *Clin Cancer Res.* 2008; 14:5649–5655. [PubMed: 18794071]
5. Bauer TW, Liu W, Fan F, et al. Targeting of urokinase plasminogen activator receptor in human pancreatic carcinoma cells inhibits c-Met- and insulin-like growth factor-I receptor-mediated migration and invasion and orthotopic tumor growth in mice. *Cancer Res.* 2005; 65:7775–7781. [PubMed: 16140945]
6. Friedl P, Wolf K. Tumour-cell invasion and migration: diversity and escape mechanisms. *Nat Rev Cancer.* 2003; 3:362–374. [PubMed: 12724734]

7. Kim TD, Song KS, Li G, et al. Activity and expression of urokinase-type plasminogen activator and matrix metalloproteinases in human colorectal cancer. *BMC Cancer*. 2006; 6:211. [PubMed: 16916471]
8. Ossowski L, Aguirre-Ghiso JA. Urokinase receptor and integrin partnership: coordination of signaling for cell adhesion, migration and growth. *Curr Opin Cell Biol*. 2000; 12:613–620. [PubMed: 10978898]
9. Riisbro R, Christensen IJ, Piironen T, et al. Prognostic significance of soluble urokinase plasminogen activator receptor in serum and cytosol of tumor tissue from patients with primary breast cancer. *Clin Cancer Res*. 2002; 8:1132–1141. [PubMed: 12006529]
10. Riisbro R, Stephens RW, Brunner N, et al. Soluble urokinase plasminogen activator receptor in preoperatively obtained plasma from patients with gynecological cancer or benign gynecological diseases. *Gynecol Oncol*. 2001; 82:523–531. [PubMed: 11520150]
11. Shariat SF, Park S, Trinh QD, Roehrborn CG, Slawin KM, Karakiewicz PI. Plasminogen activation inhibitor-1 improves the predictive accuracy of prostate cancer nomograms. *J Urol*. 2007; 178(4 pt 1):1229–1236. [PubMed: 17698116]
12. Ganesh S, Sier CF, Griffioen G, et al. Prognostic relevance of plasminogen activators and their inhibitors in colorectal cancer. *Cancer Res*. 1994; 54:4065–4071. [PubMed: 8033138]
13. Ganesh S, Sier CF, Heerding MM, Griffioen G, Lamers CB, Verspaget HW. Urokinase receptor and colorectal cancer survival. *Lancet*. 1994; 344:401–402. [PubMed: 7914317]
14. Ganesh S, Sier CF, Heerding MM, et al. Contribution of plasminogen activators and their inhibitors to the survival prognosis of patients with Dukes' stage B and C colorectal cancer. *Br J Cancer*. 1997; 75:1793–1801. [PubMed: 9192984]
15. Pyke C, Ralfkiaer E, Ronne E, Hoyer-Hansen G, Kirkeby L, Dano K. Immunohistochemical detection of the receptor for urokinase plasminogen activator in human colon cancer. *Histopathology*. 1994; 24:131–138. [PubMed: 8181805]
16. Stephens RW, Nielsen HJ, Christensen IJ, et al. Plasma urokinase receptor levels in patients with colorectal cancer: relationship to prognosis. *J Natl Cancer Inst*. 1999; 91:869–874. [PubMed: 10340907]
17. Verspaget HW, Sier CF, Ganesh S, Griffioen G, Lamers CB. Prognostic value of plasminogen activators and their inhibitors in colorectal cancer. *Eur J Cancer*. 1995; 31A:1105–1109. [PubMed: 7577001]
18. Bauer TW, Fan F, Liu W, et al. Insulinlike growth factorI-mediated migration and invasion of human colon carcinoma cells requires activation of c-Met and urokinase plasminogen activator receptor. *Ann Surg*. 2005; 241:748–756. discussion 756–758. [PubMed: 15849510]
19. Ossowski L, Reich E. Antibodies to plasminogen activator inhibit human tumor metastasis. *Cell*. 1983; 35(3 pt 2):611–619. [PubMed: 6418388]
20. Wang Y, Liang X, Wu S, Murrell GA, Doe WF. Inhibition of colon cancer metastasis by a 3'-end antisense urokinase receptor mRNA in a nude mouse model. *Int J Cancer*. 2001; 92:257–262. [PubMed: 11291054]
21. Jung YD, Liu W, Reinmuth N, et al. Vascular endothelial growth factor is upregulated by interleukin-1 beta in human vascular smooth muscle cells via the P38 mitogen-activated protein kinase pathway. *Angiogenesis*. 2001; 4:155–162. [PubMed: 11806247]
22. Yang L, Avila H, Wang H, et al. Plasticity in urokinase-type plasminogen activator receptor (uPAR) display in colon cancer yields metastable subpopulations oscillating in cell surface uPAR density—implications in tumor progression. *Cancer Res*. 2006; 66:7957–7967. [PubMed: 16912170]
23. Stoeltzing O, McCarty MF, Wey JS, et al. Role of hypoxia-inducible factor 1alpha in gastric cancer cell growth, angiogenesis, and vessel maturation. *J Natl Cancer Inst*. 2004; 96:946–956. [PubMed: 15199114]
24. Lester RD, Jo M, Montel V, Takimoto S, Gonias SL. uPAR induces epithelial-mesenchymal transition in hypoxic breast cancer cells. *J Cell Biol*. 2007; 178:425–436. [PubMed: 17664334]
25. Dallas NA, Samuel S, Xia L, et al. Endoglin (CD105): a marker of tumor vasculature and potential target for therapy. *Clin Cancer Res*. 2008; 14:1931–1937. [PubMed: 18381930]

26. Zlobec I, Minoo P, Baumhoer D, et al. Multimarker phenotype predicts adverse survival in patients with lymph node-negative colorectal cancer. *Cancer*. 2008; 112:495–502. [PubMed: 18076013]
27. Hildenbrand R, Gandhari M, Stroebel P, Marx A, Allgayer H, Arens N. The urokinase-system—role of cell proliferation and apoptosis. *Histol Histopathol*. 2008; 23:227–236. [PubMed: 17999379]
28. Lee KH, Choi EY, Hyun MS, et al. Role of hepatocyte growth factor/c-Met signaling in regulating urokinase plasminogen activator on invasiveness in human hepatocellular carcinoma: a potential therapeutic target. *Clin Exp Metastasis*. 2008; 25:89–96. [PubMed: 17992475]
29. Bauer TW, Fan F, Liu W, et al. Targeting of insulin-like growth factor-I receptor with a monoclonal antibody inhibits growth of hepatic metastases from human colon carcinoma in mice. *Ann Surg Oncol*. 2007; 14:2838–2846. [PubMed: 17653802]
30. Gray MJ, Van Buren G, Dallas NA, et al. Therapeutic targeting of neuropilin-2 on colorectal carcinoma cells implanted in the murine liver. *J Natl Cancer Inst*. 2008; 100:109–120. [PubMed: 18182619]
31. Stoeltzing O, Ahmad SA, Liu W, et al. Angiopoietin-1 inhibits vascular permeability, angiogenesis, and growth of hepatic colon cancer tumors. *Cancer Res*. 2003; 63:3370–3377. [PubMed: 12810673]

**FIGURE 1.**

Expression of urokinase plasminogen activator receptor (uPAR) on colorectal cancer (CRC) cells and in vitro effects of a monoclonal antibody (MoAb) to uPAR are shown. (A) Western blot analysis demonstrates uPAR expression in all CRC cell lines studied. (B) Effect of ATN-658 on CRC cell migration is shown. A transwell migration assay was performed on HCT-116 cells with either nonspecific immunoglobulin G MoAb or ATN-658. After 24 hours, ATN-658 significantly decreased HCT116 cell migration compared with control (55%; $P < .001$). After 48 hours, RKO and SW480 demonstrated a decrease in cell migration (90% and 35%, respectively; $P < .001$ and $P < .01$, respectively) (mean of 10 high-power fields; bars indicate the standard error).

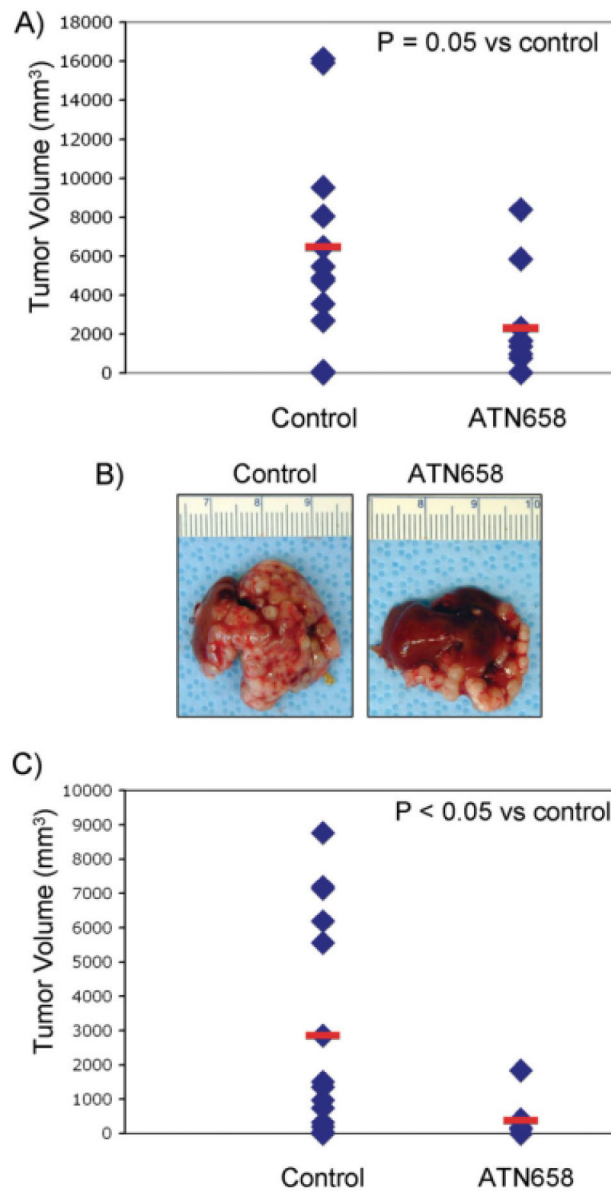


FIGURE 2.

The effect of ATN-658 on human colorectal cancer tumor growth in the liver is shown. (A) ATN-658 led to significant reductions in tumor volume versus nonspecific monoclonal antibody (MoAb) control (60% vs nonspecific MoAb-treated control group; $P = .05$) when therapy was initiated on Day 4. Tumors volumes were calculated as $(\text{length} \times 0.5) \times \text{width}^2$. Data are provided as a scatter plot of individual tumor volumes with the mean shown as a red bar. (B) Photographs of representative livers with tumor burden are shown. (C) ATN-658 lead to significant reductions in tumor and liver mass versus nonspecific MoAb control (85% vs nonspecific MoAb-treated control group; $P < .02$) when therapy was initiated on Day 12. Data are provided as a scatter plot of individual tumor volumes with the mean shown as a red bar.

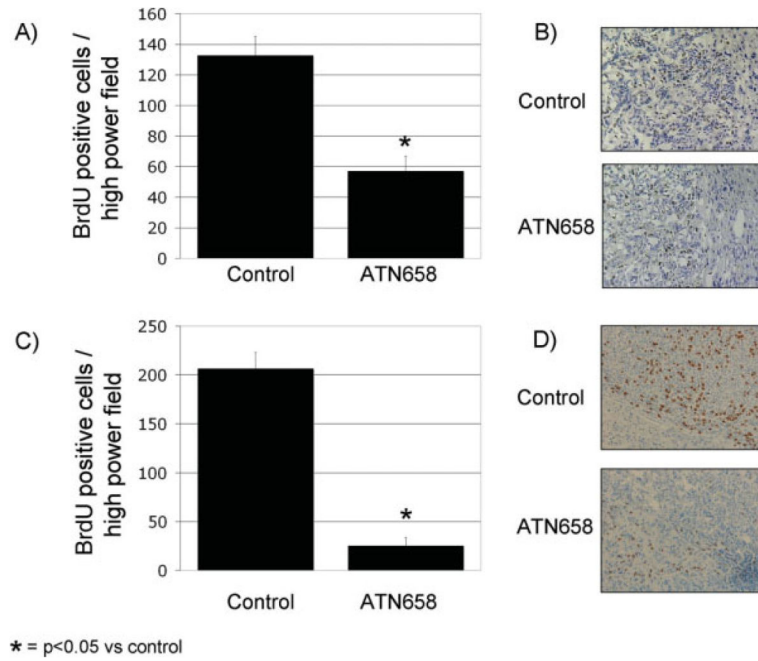


FIGURE 3.

Effect of urokinase plasminogen activator receptor monoclonal antibody (MoAb) on tumor cell proliferation in vivo is shown. Bromodeoxyuridine (BrdU) immunohistochemical (IHC) analysis of the early and late human colorectal cancer xenograft revealed numerous proliferating cells in the nonspecific MoAb (control). The number of proliferating cells in the ATN-658 group was much lower than that of the control for both the (A) small-volume ($P < .002$) and (C) large-volume groups ($P < .00001$). IHC photomicrographs at $\times 100$ magnification are also shown for BrdU in the (B) small-volume and (D) large-volume therapy groups.